13th ewtec 2019 Proceedings of the 13th European Wave and Tidal Energy Conference 1-6 Sept 2019, Naples, Italy

Economic optimisation of large scale tidal stream turbine arrays

Zoe L. Goss, Stephan C. Kramer, Alexandros Avdis, Colin J. Cotter, and Matthew D. Piggott

***Abstract*—Tidal stream electricity generation represents a relatively new technology and industry, with the world's first demonstration arrays only recently being deployed. These arrays are small scale with only three turbines installed by Nova Innovation off the coast of Shetland and four turbines installed by Meygen in Pentland Firth. Further development of the industry and the deployment of large scale arrays consisting of perhaps hundreds of turbines will only occur if these arrays can be proven to be economically viable. There is therefore a need for numerical tools that can predict and maximise the yields of large scale arrays. This can be done through modelling the hydrodynamics and optimising the number of turbines in an array as well as the location of each turbine within the array. Such tools have been developed within Thetis, a finite element coastal hydrodynamics modelling software, which enables efficient gradient-based optimisation through an adjoint model. Studies so far have shown that optimising for power alone results in a design with an unrealistically high optimal number of turbines. Optimisation functionals that introduce a penalty for the costs of a device, such as a break even power, produce arrays with a higher average power per device. The present work explores the impact of this variation in functional.**

***Index Terms*—tidal stream energy, economics, optimisation, micro-siting,**

I. Introduction

WITH a rising demand for sustainable and reliable energy, tidal energy could provide an important contribution to the future mix of renewable energy sources. The tidal resource is advantageous compared to wind and solar in terms of their predictability, due to its dependency on the understood respective motions of celestial bodies, rather than the weather. Reliability is a very important factor in the grid integration of renewable resources. There are a number of sites worldwide which have significant tidal currents that would be suitable for tidal stream generation [1]. The UK represents one such collection of locations, with its complicated bathymetry and coastline accelerating the tidal currents, resulting in a theoretical resource supply of $\approx$ 116 TWh/year [2].

Locations which are especially suitable for tidal stream energy extraction typically have coastline features that accelerate the flow velocities in the region. Draper et al. [3] characterised these features into descriptions of four generic coastal sites; a strait between two infinite ocean basins, an enclosed bay, a headland, and a strait between an island and a semi-infinite landmass. There are many tidal sites around the UK which could be described as examples of these generic models. The Pentland Firth, the site of one of the world's first tidal stream arrays, has been compared to a channel linking two infinite ocean basins. Models of the Pentland Firth by Draper et al. [4] were shown to be consistent with idealised models by Garrett et al. [5]. The Alderney Race, between Cap de la Hague in France and the Isle of Alderney, is another attractive tidal stream location as it has velocities which can exceed 5m/s and an estimated maximum average power potential of 5.1 GW [6]. The generic coastal site of a strait between an island and a semi-infinite landmass can be considered a simplification of the geometry of the Alderney Race. Power extraction by narrow arrays (similar to tidal fences) spanning across the strait in this type of generic coastal site were investigated by Peréz-Ortiz et al. [7]. This work replicates the simplified setup used by Peréz-Ortiz et al. and extends upon it by investigating optimisation of larger scale arrays. To model a simple setup similar in dimensions to the potential tidal sites in the Alderney Race, the arrays tested in this work have a width and length of comparable size, rather than narrow arrays such as tidal fences.

Tidal stream energy is an emerging industry, with the worlds first arrays only recently installed, each with very few tidal devices deployed. Nova Innovation have an array of three turbines off the coast of Shetland, while MeyGen in the Pentland Firth have installed four turbines. Tidal stream arrays will need to consist of many more devices if they are to make a substantial impact on meeting clean energy targets. Potential sites, such as the Alderney Race, may consist of arrays of up to hundreds of turbines. At these larger scales the design of the arrays is non-trivial. Tidal site developers will need to find the optimal locations of devices within their tidal plots and also decide on the most appropriate number of turbines to use in order to balance out maximising revenue from power generations with minimising the costs of the array. At this early stage in the tidal industry these design decisions are best

The ID number of this paper is 1598, submitted under the conference track 'Economical, social, legal and political aspects of ocean energy' (ESP). Z. L. Goss acknowledges the support of an EPSRC PhD studentship, through the Mathematics of Planet Earth CDT. M. D. Piggott acknowledges the support of EPSRC under grants EP/M011054/1 and EP/R029423/1.

Z. L. Goss is at the Department of Earth Science and Engineering, Imperial College London, London, UK, SW7 2AZ (e-mail: zg811@imperial.ac.uk

S. C. Kramer is at the Department of Earth Science and Engineering, Imperial College London, London, UK, SW7 2AZ (e-mail: s.kramer@imperial.ac.uk

A. Avdis is at the Department of Earth Science and Engineering, Imperial College London, London, UK, SW7 2AZ (e-mail: a.avdis@imperial.ac.uk

C. J. Cotter is at the Department of Mathematics, Imperial College London, London, UK, SW7 2AZ (e-mail: colin.cotter@imperial.ac.uk

M. D. Piggott is at the Department of Earth Science and Engineering, Imperial College London, London, UK, SW7 2AZ (e-mail: m.d.piggott@imperial.ac.uk

aided through numerical tools which can model the hydrodynamics in the region and optimise the number and location of turbines.

Previous work has demonstrated the ability of coastal ocean modelling packages such as *Thetis* [8] (http://thetisproject.org/) utilising finite-element methods along with an adjoint facilitating gradient-based optimisation to solve the hydrodynamics and predict and optimise array yields [9]–[12]. These approaches have then been applied to realistic case studies such as the Alderney Race [13], [14]. However, it has been shown that optimisation for power alone can produce array designs with impractically high numbers of turbines and that the functional for optimisation must be carefully chosen to reflect the balance between an investor's desire to maximise power generation while also keeping costs to a minimum.

The following sections outline how the simplified representative model for initial testing in this work is set up, how the array of turbines is represented in the model and how the array design is then optimised. It is then demonstrated how the optimal design varies with different choices of functional as more importance is placed on minimising costs vs. maximising power generation.

II. Methodology

This section first describes the setup of a tidal model of a channel between an island and a larger landmass. First the numerical model is outlined, then the spatial and temporal discretisation options, and finally the tidal forcing of the model are presented.

A. Numerical model

The tidal modelling in this work is carried out using the depth-averaged shallow water configuration of *Thetis*, a flexible finite-element based coastal ocean model implemented in Python, using the *Firedrake* framework (https://www.firedrakeproject.org/) along with Unified Form Language (UFL) [15] for high level code generation. Simulations of flow in a channel are performed by solving the non-conservative form of the nonlinear shallow water equations

$$\begin{aligned} \frac{\partial \eta}{\partial t} + \nabla \cdot (h\mathbf{u}) &= 0, \\ \frac{\partial \mathbf{u}}{\partial t} + \mathbf{u} \cdot \nabla \mathbf{u} - \nu \nabla^2 \mathbf{u} + g \nabla \eta + C_d \frac{|\mathbf{u}|\mathbf{u}}{h} &= 0, \end{aligned} \tag{1}$$

where t is time, $\mathbf{u} = (u, v)$ is the 2D depth-averaged velocity vector, η is the free surface perturbation, g is acceleration due to gravity, h is the total water depth. C_d is a dimensionless quadratic drag coefficient for seabed friction, set to 0.0025, ν is the kinematic viscosity of the fluid and is set to a value of $0.0001 m^2 s^{-1}$, to act as closure for sub-grid scale turbulence. Coriolis, atmospheric pressure, wind & wave conditions are not included in this simplified model.

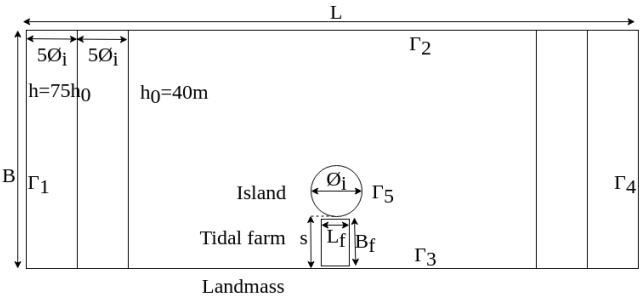

Fig. 1. Geometry for a model of flow through a channel with an island of diameter $\emptyset_i = 2000m$ and a tidal site of area $A_f = B_f \times L_f$ where turbines can be added. The depth is increased linearly from h_0 to $75h_0$ to mimic the conditions at the continental shelf.

B. Model parameterisation

Fig. 1 depicts the geometry of this simple model of flow past an island near a far larger landmass, based on the setup from [7]. The flow is simulated through a channel that is $L = 140km$ long and $B = 40km$ wide. A circular island with a diameter of $\emptyset_i = 2km$ and a minimum distance to the southern landmass of $s = 2km$ is located in the middle of the channel.

When optimising the design of a tidal array in the region, the turbines are constrained to only occupy a rectangular farm area, A_f, which represents a typical lease plot that a tidal developer may be allowed to deploy turbines within. The dimensions were chosen to mimic those in the Alderney Race, with the maximum length of the farm $L_f = 1km$ around half the length of the island, and the maximum width of the farm spanning across the whole width of the strait with a $0.4km$ buffer on either side, such that the width $B_f = 1.92km$.

The water depth is set to $h_0 = 40m$ across the majority of the channel, but linearly increases to $75h$ in the streamwise direction from $20km$ to $10km$ away from the eastern and western boundaries, as shown in Fig. 3. This mimics conditions at the edge of the continental shelf and helps prevent spurious reflections at the boundary.

C. Tidal forcing and boundaries

There are five boundaries which define the domain as shown in Fig. 1. First are the solid boundaries at the northern and southern sides of the domain, Γ_2 & Γ_3, where a free slip boundary conditions is applied, to correspond to a semi-infinite landmass, e.g. the shores of France and the UK. Likewise, a free slip boundary condition is applied to the solid boundary of the island, Γ_5.

The open boundaries on the western and eastern side of the channel, Γ_1 and Γ_4 respectively, are used to force the flow in the model. Zero surface elevation is prescribed at Γ_4 and free surface elevation at Γ_1, with M2 tidal forcing of the form

$$\delta_1 = a_0 a \sin(\omega_t t) \tag{2}$$

where amplitude $a = 3m$ and frequency $\omega_t = 1.41 \times 10^{-4} rad/s$. The additional multiplier $a_0 = 0.5(1 - \cos(\omega_t t/4))$ is used to ramp up the tidal signal over

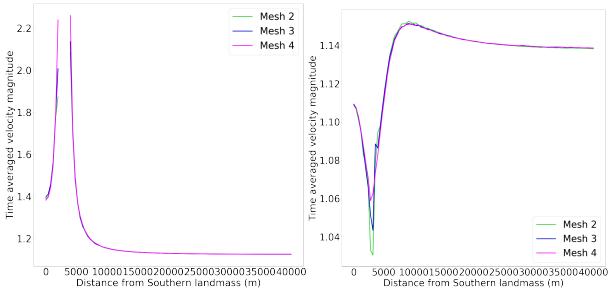

Fig. 2. Mesh convergence of the stream-wise time-averaged velocity profile at for (a) a transverse cross section through the island centre and (b) a cross section through $2\emptyset_i$ East of the island centre.

TABLE I
THE SPATIAL DISCRETISATIONS AND NUMBER OF ELEMENTS USED IN MESH CONVERGENCE STUDIES.

Mesh	Element edge length				Elements
	Landmass	Strait	Island	North	
1.	$\pi\emptyset_i/6$	$\pi\emptyset_i/6$	$\pi\emptyset_i/12$	$\pi\emptyset_i$	4736
2.	$\pi\emptyset_i/6$	$\pi\emptyset_i/6$	$\pi\emptyset_i/28$	$\pi\emptyset_i$	5010
3.	$\pi\emptyset_i/17$	$\pi\emptyset_i/28$	$\pi\emptyset_i/36$	$\pi\emptyset_i$	12200
4.	$\pi\emptyset_i/17$	$\pi\emptyset_i/36$	$\pi\emptyset_i/76$	$\pi\emptyset_i$	14504

the first two tidal cycles. The model is allowed to spin up for an additional two tidal cycles and any time averages are only taken over the final three cycles.

D. Discretisation of the model

A Crank-Nicolson time stepping method is employed for temporal discretisation, with $\Delta t = 800s$ used in the models presented below. The convergence of the velocity solution for different time step sizes, from $\Delta t = 1600s$ to $\Delta t = 100s$, were analysed and it was found that time step independence is achieved even at higher values of Δt. Fig. 2(a) shows the velocity profile at a transverse cross section through the island centre and Fig. 2(b) shows it for $2\emptyset_i$ east of the island centre.

The finite-element discretisation utilised in this work is based on piecewise-linear, discontinuous basis functions for both the velocity and free surface fields (the $\mathrm{P_{1DG}} - \mathrm{P_{1DG}}$ velocity-pressure finite element pair). There are four boundary regions upon which the element edge length is specified, in order to define the unstructured triangular mesh. It is set to a coarser value on the northern solid boundary, slightly finer along the southern landmass, even finer in the region of the southern landmass that is within $2\emptyset_i$ from the island (to resolve the flow in the strait better), and at its finest around the island boundary. Furthermore in the tidal farm area a fine grid of 20 by 40 right-angled isosceles triangles is used in all meshes.

Convergence of the velocity using four different mesh resolutions was tested, as defined in Table I. Fig. 2(a) shows that the velocity profile remains very similar for all meshes, except Mesh 1, which was found to be unstable. The optimisations considered in the following sections therefore all use Mesh 2.

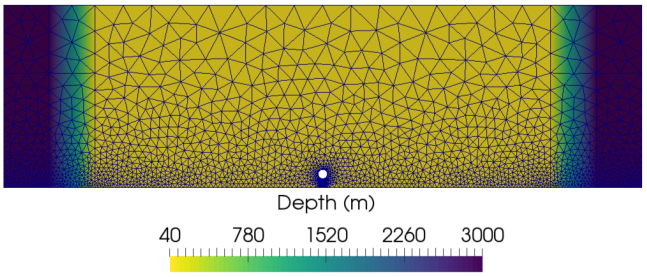

Fig. 3. Multi-scale unstructured computational mesh and depths across the domain.

III. TURBINE REPRESENTATION

Two main approaches for finding optimal locations for individual devices within an array (turbine micro-siting) are available in *Thetis*. [9], in the earlier implementation OpenTidalFarm, used a discrete approach where turbines were individually resolved and each represented a friction 'bump' function, and the location of the centres were optimised. That approach requires relatively high mesh resolution in order to 'resolve' individual turbines and hence leads to high computational costs. [10] proposed a continuous approach where a spatially varying turbine density field is instead optimised. This has the advantage that a coarser mesh resolution can be applied. It has the additional benefit that the number of turbines and location are optimised together, whereas the discrete approach would require a secondary optimisation loop [11] to achieve this which would result in additional computational costs. However, the continuous modelling approach does not account for turbine-scale losses, so results should be viewed as an upper limit to power extraction. [10] demonstrated that, once discretised to obtain individual turbines locations that meet the prescribed density, the resulting array designs from both approaches are similar. Therefore the discrete method is used in the following sections.

The presence of turbines in the farm area, A_f, is modelled through the addition of an enhanced bottom friction term,

$$\frac{c_t}{\rho H}||\mathbf{u}||\mathbf{u}, \tag{3}$$

on the left hand side of the Shallow Water Equations (1). The coefficient in the bottom friction term corresponds to the spatially varying turbine density via

$$c_t(d(x)) = \frac{1}{2}C_T A_T d(x), \tag{4}$$

where $d(x)$ is the turbine density field, to be optimised within A_f and set to zero outside it. A_T is the swept area of the turbines, which are assumed to take a value corresponding to 16m diameter turbines in this study. An upper limit on $d(x)$ is imposed and is based on a maximum turbine density which would be commensurate with a minimum inter-device spacing of 2.5 turbine diameters centre-to-centre laterally and 5 turbine diameters in the stream-wise direction. This upper limit was chosen to represent a high but still plausible density of turbines.

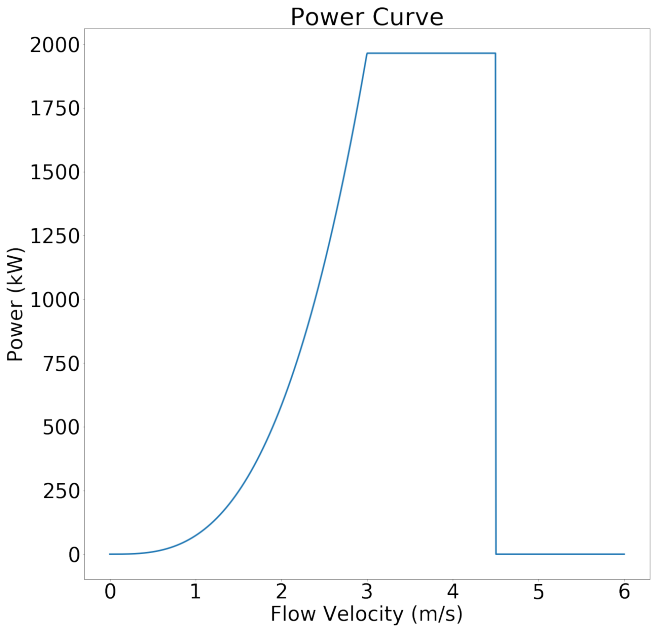

Fig. 4. Power curve of a typical generic tidal turbine assumed for this work.

C_T is the turbine thrust coefficient, set to follow the power curve shown in Fig. 4, with an assumed cut-in speed of $0m/s$, a rated speed of $3m/s$ (at which $C_T = 0.8$) and a cut-out speed of $4.5m/s$.

The number of turbines, N, can be found by integrating the density over the array area A_f,

$$\int_{A_f} d(x)\, dx = N_t. \tag{5}$$

Similarly, the power is found by integrating over the array area A_f to obtain

$$P = \rho \int_{A_f} c_t(d(x))||\mathbf{u}||^3\, dx. \tag{6}$$

This quantity is then averaged over all time steps in the last three simulated tidal cycles, with a ramp up time of two tidal cycles and a spin up of two more, to obtain the average power.

E. Adjoint-based optimisation

The following sections present the results obtained when optimising the array layout, using $d(x)$ as the control parameter, to maximise average power or other profit based metrics for the array. The array is initially configured with a density of zero turbines everywhere. At each iteration of the optimisation the forward model is run with the corresponding turbine friction coupled to the hydrodynamics and the power and functional estimates are recalculated. An adjoint calculation is then performed (via http://pyadjoint.readthedocs.io/ library), to enable gradient-based optimisation of the turbine density. The adjoint model allows for the calculation of the sensitivity of the functional to changes in $d(x)$, while taking into account the associated changes in hydrodynamics, by determining the gradient of the functional, J. An L-BFGS-B based optimisation algorithm then uses this sensitivity information to update the turbine density field. The optimisation iterations converge on an optimal array design and the algorithm is completed. For the configuration considered in this work this typically occurs within 5 to 20 iterations, depending on the choice of functional.

The choice to model turbines through a density rather than discretely means that individual wake effects are not resolved, so power extraction estimates are an upper bound. However, the density coupling with the hydrodynamics does account for larger scale blockage effects. As shown in [13], increasing the global blockage, by having turbines stretch across the width of the strait, may at first increase the power per turbine due to restricting array by-pass. However, when the turbine density is too high, global blockage may reduce the overall power generated since the corresponding friction becomes so high it leads to a reduction in the channel flow rate [16].

F. Choice of (economic) functional

Previous studies have shown that the the optimal array design, when the functional is power alone, tends to result in array design with an impractically high number of costly turbines which only generate a little bit more power than array designs with far fewer turbines [13], [14]. Financially it is far better to design a smaller, cheaper array where the power per device ($ppd = AvgPower/n_t$) is much higher, so that with time they generate enough to cover the costs of the array. To address this problem, a break even power (BEP) is included in the functional which accounts for the money earned per unit of power generated, but also spent per device installed. This effectively penalising the additional of turbines which no not generate enough power.

The BEP can be thought of as the amount a turbine needs to generate on average in order for it to be worth the cost of installing. It is the average power over all turbines that needs to be generated in order for the array to break even over its lifetime, such that

$$\sum_{y=0}^{n} P_{BE} \times T_e \times t_y \times n_t - C_y = 0, \tag{7}$$

where P_{BE} is the BEP in MW, T_e is the electricity tariff, i.e. the price per MWh the electricity generated is sold at, y is the year the costs are being evaluated over, n is lifetime of the array in years, t_y is the number of hours generating in a year and C_y is the sum of all array costs incurred in year y. For an array that takes one year to build, $t_0 = 0$, as there is no power generation during construction, and C_0 is the Capital Expenditure (CAPEX), which are the expenses incurred to acquire or upgrade physical assets. In the case of an array this includes the costs of the devices, the electrical equipment and cost of installation. Similarly $C_{y\geq 1}$ is the Operational Expenditure (OPEX), which are the funds used for normal business operations measured on an annual basis. For an array of turbines this may include standard inspections, maintenance, repairs and costs of vessels and staff to perform these tasks.

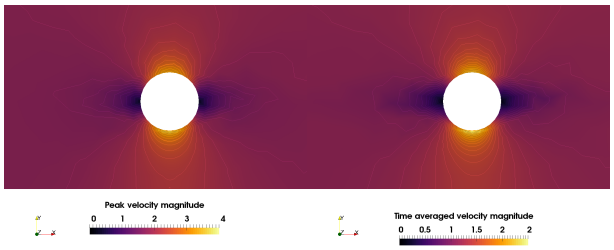

(a) (b)

Fig. 5. (a) Peak velocity around island; (b) time averaged velocity around island, without the presence of turbines.

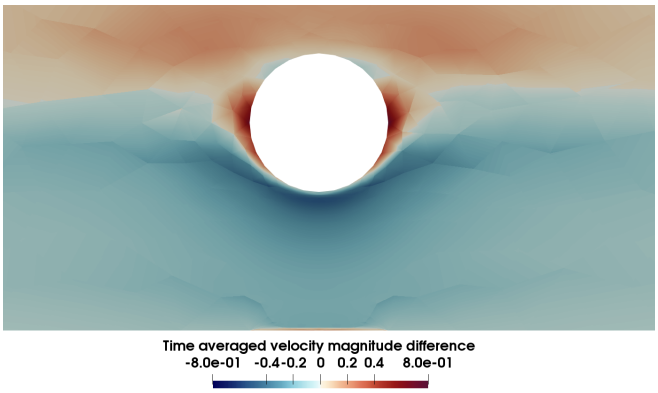

Fig. 6. Velocity difference around island after adding a full array of turbines.

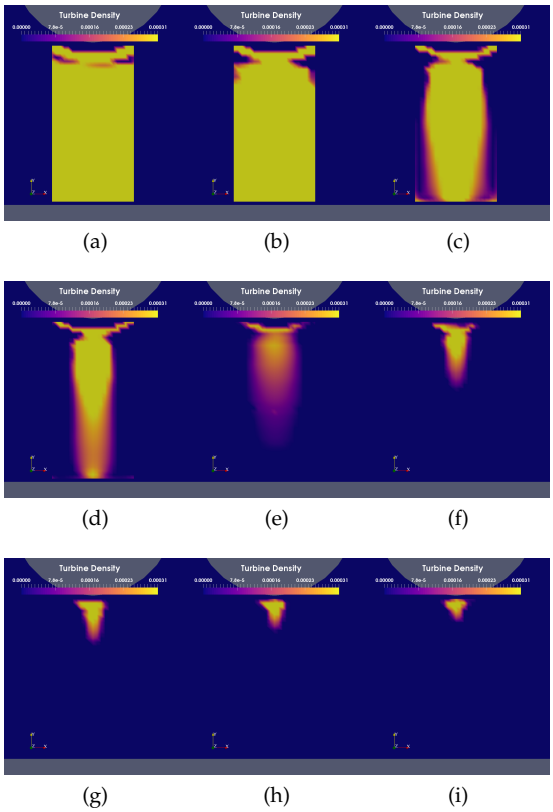

(a) (b) (c)

(d) (e) (f)

(g) (h) (i)

Fig. 7. Optimal array for break even power of (a) 0, (b) 100, (c) 200, (d) 300, (e) 400, (f) 500, (g) 600, (h) 700, and (i) 800 kW.

The four 1.5MW turbines installed by MeyGen in Pentland Firth have a contractual capacity factor, C_p, of 0.38 [17], meaning they would expect their turbines to generate at least 570kW on average throughout the year to be viable. To test the impact that including the cost of turbines through an effective break even power has, the results below present the variation in optimal design for BEP's in the range from 100 to 800kW, compared to optimising for power alone (which is of course equivalent to specifying $P_{BE} = 0kW$).

IV. Results

First, to analyse the resource, the flow through the channel without the presence of turbines was investigated. Fig. 5 shows the peak velocity and time-averaged velocity magnitude across a tidal cycle. They show why straits between an island and a landmass are attractive sites for tidal turbine arrays, with flows of around double the magnitude of the rest of the channel for the configuration considered here.

Fig. 6 shows that with the presence of a full array of turbines (i.e. with the turbine density set at its maximum allowed value over the entire array area) the velocity through the strait slows down, especially close to the island. It can also be seen that the bypass flow, on the Northern side of the island, shows corresponding increases in magnitude, from 1.5m/s to 2m/s. This is an example of global blockage and could indicate that islands hoping to best exploit their tidal resource should investigate installing (limited sized) arrays both in the strait and offshore in response to blockage effects. Furthermore, the flow is greatly accelerated to the immediate East and West of the island, from around 0m/s to 0.8m/s. This may be something to consider as part of the Environmental Impact Analysis of a new array, if there are any site of ecological interest, such as wildlife taking advantage of the previously still waters in the region, or if erosion is a concern.

Fig. 7 shows the optimal array designs obtained when optimising for functionals of the form $J = P_{avg} - P_{BE} \cdot n_t$, where $P_{BE} \in [0, 800]kW$. There are a few notable trends in the presented results, many of which are arguably intuitive. Firstly, as P_{BE} increases, the optimal n_t decreases, and the location of the remaining turbines transitions from being spread across the majority of A_f to just the region with the fastest flows – closest to the island.

Fig. 8 shows two examples of how the array characteristics change with each iteration of the optimisation until the optimal array design is reached. The process is shown for two functionals; first when optimising for power alone and second when optimising with a break even power of 400kW. It can be seen that when optimising for power alone the power increases with each iteration until it converges on an optimum power, however the power per device is not especially high. When optimising with a break even power, the value of the functional, $J = P - 400 \cdot n_t$, increases with each iteration, whereas the net power decreases as turbines are removed to keep the penalty from the turbine costs down. This design results in a much higher power per device.

Fig. 9(a) shows how the average power of the array and the average power per device (P/n_t) varies in

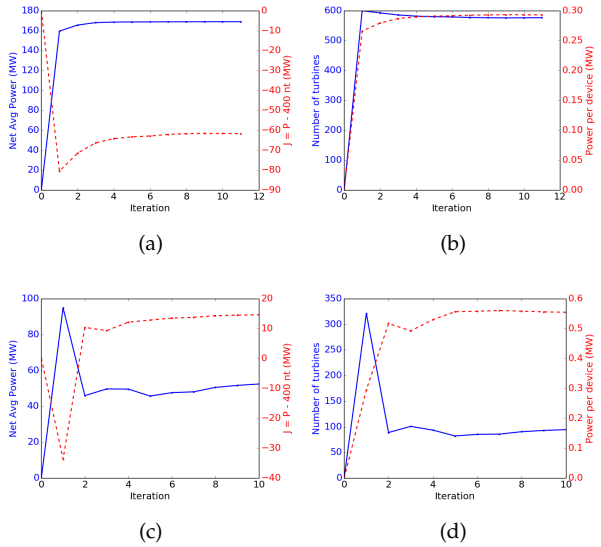

Fig. 8. Comparison between tidal farm parameters (number of turbines, net power, power per device) per iteration for the optimisation of a farm when using power alone as the functional, $J = P$, (a) & (b), vs using $J = P - 400 \cdot n_t$, (c) & (d).

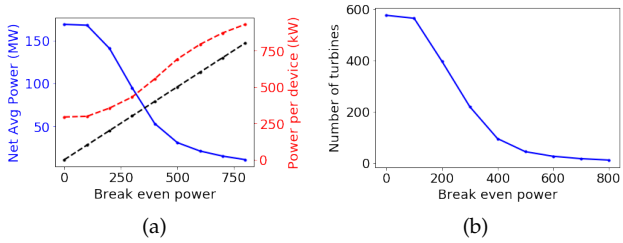

Fig. 9. Variations in the average power generated and the number of turbines for the optimal design as the BEP is increased.

the optimal design for different break even powers. When adding a proxy for the cost of turbines into the functional, through the use of a break even power, the balance of priorities between maximising total power generation vs keeping the costs down is shifted. This leads to a decrease in total power from 169MW to 11MW generated as the break even power is increased from 0 to 800kW. However, as shown in Fig. 9(b) this is accompanied by a drop in number of turbines from 577 to just 12. Furthermore the power generated per device triples from 0.3MW to 0.9MW through these range of functionals. This confirms that the optimisation is indeed respecting what is being asked of it through the functional definition. It also implies that the arrays designed with a higher break even power are providing a better return on the costs invested in installing those turbines, provided that the electricity generated is enough to cover the fixed costs of the array as well.

The power per device always remains higher than P_{BE} in the optimal design. It is easy to see why this is the case by rearranging the functional and noting that any solution where the functional is negative cannot be an optimal one since a solution with no turbines will always obtain a functional of zero. Therefore $J = P_{avg} - P_{BE} \cdot n_t \geq 0$ implies that $P_{BE} \geq P_{avg}/n_t$.

It is also noticeable that the array properties shown

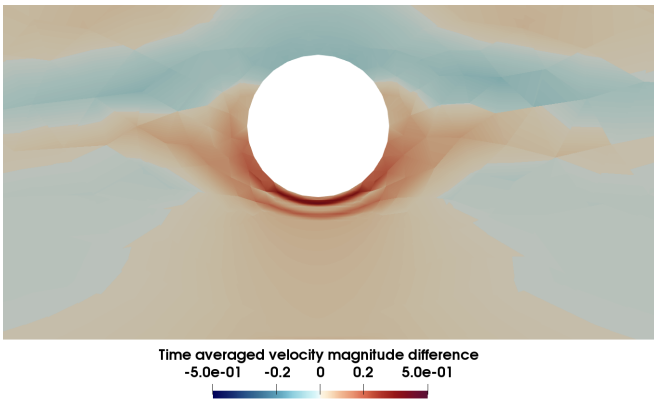

Fig. 10. Velocity difference around island – the array density optimised for power alone minus the case of an array of maximum turbine density everywhere.

in Fig. 9 are more sensitive to changes in the region $200kW \leq P_{BE} \leq 600kW$ than they are for break even powers above and below that range. Therefore array designers which require a break even power in a given range should be careful about their choice of functional.

There are some arguably less intuitive results in the optimisation of the array design. The shape of the resulting optimal arrays in particular is notable, especially the regions which contain no turbines even when optimising for power alone. These results can be best understood by viewing the difference in time-averaged velocity magnitude before and after adding turbines in that area, in order to investigate the impact the turbine positioning has on global blockage. Fig. 10 shows the difference between the time-averaged velocity field for a simulation with the array density obtained by optimising for power alone, shown in Fig. 7(a), minus the velocities with the array density set to its maximum value everywhere within A_f.

As can be seen in Fig. 7(a), to maximise power the optimal density is maximal almost everywhere except in a small semi circle just south of the island and in another ring shape just below that. Fig. 10 shows that the removal of turbines in those locations increases the flow through the strait by up to 0.6m/s and decreases the bypass flow by a similar amount. This appears to be because placing maximal turbine density everywhere in the region with the highest flow speeds leads to so much global blockage and bypass flow around the island that the array generates less power overall. With 14 fewer turbines the array optimised for power generates 5.3% more power than an array which has maximal turbines everywhere, with an increase from 159MW to 168M.

Due to the near symmetry of the results obtained here, qualitative changes in the optimal array design as the break even power is varied can be visualised by plotting the optimal turbine density along the vertical centre line of the array. At high break even powers the density is highest close to the island, as the array requires that all the turbines it can afford be in the fastest flowing regions. As the break even power is decreased more turbines can be afforded in the optimal

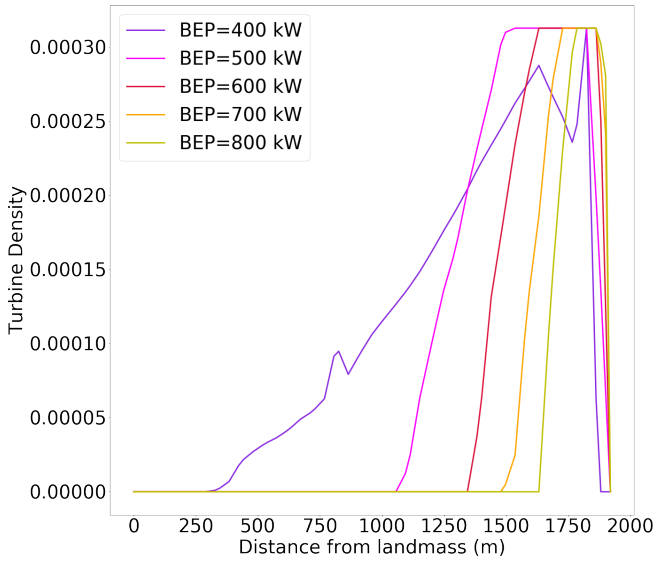

Fig. 11. The optimal turbine density along the vertical centre line (from 0m from the Southern Landmass to 2000m at the most Southern part of the island) of the array as break even power increases.

design and they spread out further South, while maintaining maximal density closest to the island. However, we can observe a qualitative change as the break even power decreases from 500 to 400kW, where it is no longer optimal to have maximum turbine density close to the island, and instead the optimal design has more turbines spread across the width of the strait. This effective decrease in costs means the array can now begin to start mimicking a barrage or fence and seek to exploit the benefits that can be realised through blockage control. This design strategy resembles some of the results found when optimising tidal arrays in the Alderney Race, where arrays which spread across the whole width of the Race were able to capture the resource more effectively. Further investigation is required to gain a more in-depth understanding of this potentially important result.

V. Discussion & Further Work

These results show that optimal array design is greatly dependent on the importance placed on power generation maximisation vs cost minimisation. However, it appears that sensitivity to this balance of priorities is heightened for medium-range break even power values. Array designers should be aware of this region of greater sensitivity when trying to evaluate the impact of uncertainty on the optimal design.

It can also be seen that global blockage can have an important effect on optimal array designs, especially for larger scale arrays. This shows the importance of modelling the larger channel region and not just the strait itself, and the need to use models where the hydrodynamics and the presence of turbines are fully coupled. However, it should be noted that these results were obtained using a turbine density approach only which although accounting to global blockage effects does not include the effects of local blockage. Previous work by Funke et al. [10] has found that large scale arrays can be efficiently optimised by using the continuous approach to obtain an optimal turbine density as a first guess at an optimal layout and an appropriate total number of turbines, then a discrete approach which represents individual turbines can be used to model and optimise the micro-siting of turbine locations using that density as an initial guess at an optimal array layout. A study should be run using the discrete approach to modelling turbines to compare how the individual resolving of turbines and local blockage effects impact on these results.

The results presented here are for the free slip scenario only. Work by Peréz-Ortiz et al. [7] showed that free slip boundary conditions tend to over-estimate the power generation, whereas no slip conditions tend to under-estimate it and that the true answer is likely between the two. Further work should recompute the results when using a no slip boundary condition and compare the two models as an upper and lower bound. Robin conditions could also be applied to interpolate between no slip and free slip and parameterize the boundary layer. These further studies should also include more realistic representations of turbulent mixing through the use of a more sophisticated turbulence closure model.

While break even power can be seen as a simple and intuitive way to bring economical considerations into array optimisation, there are a number of ways this could be advanced. One assumption in the results presented above is that the break even power is independent of the number of turbines. In practice there may be economies of scale such that the break even power decreases as the number of turbines increases; in a simple linear case $P_{BE} = A - B \cdot n_t$ where $A \ll B$. When added to the functional this would introduce a quadratic term, $J = P_{avg} - A \cdot n_t + B \cdot n_t^2$. This could have the effect of weighting the design in favour of larger scale arrays.

There are also a number of different economic metrics that could be optimised for instead which would give a more holistic view of the balance of different costs and priorities. Optimising the Levelised Cost of Energy (LCOE), rather than simply power alone or a simple function of power and number of devices, enables the inclusion of far more variables, such as initial costs, time-dependent costs, as well as those which vary depending on the number and location of devices. The LCOE is a useful metric for investors and minimising it would help ensure a good return on investment. This current work is in the process of being extended by incorporating a model for LCOE and using it as the functional to be optimised when designing a tidal turbine array.

Furthermore, Vazquez et al. [18] showed that estimates of capital costs of tidal energy projects based on installed power fail to capture the sensitivity to site-specific characteristics such as water depth and distance to shoreline. These variations could be included in more advanced economic models, such as LCOE, where the sum of the costs include costs that vary with number of turbines, distance of those turbines to shore, and the water depth they are installed in.

REFERENCES

[1] R. Rosli and E. Dimla, "A review of tidal current energy resource assessment: Current status and trend," in *2018 5th International Conference on Renewable Energy: Generation and Applications (ICREGA)*. IEEE, 2 2018, pp. 34–40. [Online]. Available: https://ieeexplore.ieee.org/document/8337585/

[2] Crown Estate, "UK Wave and Tidal Key Resource Areas Project Executive Summary," 2013. [Online]. Available: https://www.thecrownestate.co.uk/media/5478/uk-wave-and-tidal-key-resource-areas-technological-report.pdf

[3] S. Draper, "Tidal Stream Energy Extraction in Coastal Basins," Tech. Rep., 2011. [Online]. Available: https://pdfs.semanticscholar.org/d37d/300d76bed70c757cee2d403f6e6ce9143a21.pdf

[4] S. Draper, T. A. Adcock, A. G. Borthwick, and G. T. Houlsby, "Estimate of the tidal stream power resource of the pentland firth," *Renewable Energy*, vol. 63, pp. 650 – 657, 2014.

[5] C. Garrett and P. Cummins, "The power potential of tidal currents in channels," *Proceedings of The Royal Society A: Mathematical, Physical and Engineering Sciences*, vol. 461, pp. 2563–2572, 08 2005.

[6] D. S. Coles, L. S. Blunden, and A. S. Bahaj, "Assessment of the energy extraction potential at tidal sites around the Channel Islands," *Energy*, vol. 124, pp. 171 – 186, 2017.

[7] A. Prez-Ortiz, A. G. Borthwick, J. McNaughton, H. C. Smith, and Q. Xiao, "Resource characterization of sites in the vicinity of an island near a landmass," *Renewable Energy*, vol. 103, pp. 265 – 276, 2017. [Online]. Available: http://www.sciencedirect.com/science/article/pii/S0960148116309740

[8] T. Kärnä, S. C. Kramer, L. Mitchell, D. A. Ham, M. D. Piggott, and A. M. Baptista, "Thetis coastal ocean model: Discontinuous Galerkin discretization for the three-dimensional hydrostatic equations," *Geoscientific Model Development*, vol. 11, no. 11, pp. 4359–4382, 2018.

[9] S. Funke, P. Farrell, and M. Piggott, "Tidal turbine array optimisation using the adjoint approach," *Renewable Energy*, vol. 63, pp. 658–673, March 2014.

[10] S. W. Funke, S. C. Kramer, and M. D. Piggott, "Design optimisation and resource assessment for tidal-stream renewable energy farms using a new continuous turbine approach," *Renewable Energy*, vol. 99, pp. 1046 – 1061, 2016.

[11] D. Culley, S. Funke, S. Kramer, and M. Piggott, "Integration of cost modelling within the micro-siting design optimisation of tidal turbine arrays," *Renewable Energy*, vol. 85, 01 2016.

[12] ——, "A surrogate-model assisted approach for optimising the size of tidal turbine arrays," *International Journal of Marine Energy*, vol. 19, pp. 357 – 373, 2017.

[13] Z. L. Goss, M. D. Piggott, S. C. Kramer, A. Avdis, A. Angeloudis, and C. J. Cotter, "Competition effects between nearby tidal turbine arrays-optimal design for Alderney Race," Tech. Rep., 2018.

[14] Z. L. Goss, M. D. Piggott, and S. C. Kramer, "An English Channel Model for the Optimisation of Tidal Turbines in the Alderney Race," Tech. Rep., 2018.

[15] M. S. Alnæs, A. Logg, K. B. Olgaard, M. E. Rognes, and G. N. Wells, "Unified form language: A domain-specific language for weak formulations of partial differential equations," *ACM Trans. Math. Softw.*, vol. 40, no. 2, pp. 9:1–9:37, Mar. 2014.

[16] R. Willden, T. Nishino, and J. Schluntz, "Tidal stream energy: designing for blockage," *Oxford Tidal Energy Workshop*, pp. 27–28, 04 2014.

[17] Meygen Ltd, "Lessons Learnt from MeyGen Phase 1a Part 1/3: Design Phase Lessons Learnt from MeyGen Phase 1a Part 1/3: Design Phase LESSONS LEARNT FROM MEYGEN PHASE 1A. PART 1/3: DESIGN PHASE CONTENTS," Tech. Rep., 2017. [Online]. Available: https://tethys.pnnl.gov/sites/default/files/publications/MeyGen-2017-Part1.pdf

[18] A. Vazquez and G. Iglesias, "Capital costs in tidal stream energy projects a spatial approach," *Energy*, vol. 107, pp. 215–226, 07 2016.